SAND79-1002
Unlimited Release

UC-35

Prediction of Ground Motion From Nuclear Weapons Tests at NTS

Luke J. Vortman

SF 2900 Q(7-73)

SAND79-1002
Unlimited Release
Printed November 1979

Distribution
Category UC-35

PREDICTION OF GROUND MOTION FROM NUCLEAR WEAPONS TESTS AT NTS

Luke T. Vortman
Experiments Planning Division 1111
Sandia Laboratories
Albuquerque NM 87185

ABSTRACT

Ground motion data from underground nuclear detonations during FY78 were added to data from earlier detonations; the data were used to formulate a tentativ equation for predicting ground motion at the Nevada Test Site. Additional measurements to explore an unexplained seismic anomaly in Jackass Flats are described. Methods used in automatic processing of ground motion data are explained.

ACKNOWLEDGMENTS

Recent ground motion measurements were made by Henry Stuckert and John Dickinson. J. W. Long was responsible for automated data processing.

CONTENTS

TABLES

ILLUSTRATIONS

ILLUSTRATIONS (cont)

PREDICTION OF GROUND MOTION FROM NUCLEAR WEAPONS TESTS AT NTS

Introduction and Purpose

This report covers the FY78 activities of Subtask 1.1, Data Processing and Analysis, and Subtask 1.2, Weapons Test Ground Motion Measurements of the Nevada Nuclear Waste Storage Investigation (NNWSI). Weapon testing is a continuing activity at the Nevada Test Site (NTS) at the present time, and even though a Comprehensive Test Ban (CTB) Treaty were implemented, testing could be expected to continue either after expiration of a fixed-term treaty or abrogation of the treaty. Further, it is reasonable to expect that testing could resume at yields above the present 150 kt threshold to those maximum yields for each of the testing areas set by the potential for off-site damage.

A terminal waste facility located at or near NTS must be designed to withstand ground motion from nuclear tests at whatever level and safety factor is specified by NRC. To provide design criteria for such a facility it is necessary to be able to predict the ground motion as a function of weapon yield and distance from the source, and to be able to assess the level of confidence in the prediction methods. The development of prediction techniques from measured ground motion data is the principal purpose of Subtask 1.1. Data from past tests are predominantly of surface motion and are useful in the development of surface motion-distance-yield relationships. The locations at which measurements have been made are seldom at or near potential storage sites.

It is the purpose of Subtask 1.2 to acquire data from continuing tests for inclusion in the data bank being processed and analyzed by Subtask 1.1. These data come from measurements made near potential sites and

include measurements at depth where existing holes permit. The newly acquired data come from tests with yields below the 150 kt limit of the Threshold Test Ban (TTB) Treaty; hence, only the earlier data are applicable in the event that the TTB or any other treaty were terminated and testing resumed at the higher limit. The limits currently set for four of the active testing areas are about 1000 kt for the Pahute Mesa area, 700 kt for the Buckboard Area, and 250 kt for Frenchman Flat and Yucca Flat.

Just as it is important that a storage facility not be damaged by ground motion from underground nuclear tests, so also is it important that a facility not be located where its vulnerability to ground motion would place an unacceptable inhibition on the Weapons Test Program's ability to conduct tests. The prediction methods developed by Subtask 1.1 serve equally well for the evaluation of the impact of an NTS storage facility on the testing program.

Measurements Made in FY78

Table 1 lists the stations at which ground motion measurements are being made. Also shown in the table are the coordinates, the elevation of surface stations and the down-hole station (where there is one), the depth of the hole, the medium, and the date installed. Where a station has been deactivated, the date of deactivation is also indicated. Figure 1 shows the locations of each of these stations on a map of NTS. At each surface or down-hole station is a canister containing three orthogonally-oriented accelerometers. The output of the accelerometers is passed through signal conditioning equipment to a transmitter which transmits information from each gage over a separate subcarrier frequency to a receiver at one of the central recording facilities where it is recorded in analog form on magnetic tape. Data are digitized for further processing as described below. All stations have amplifiers, some of which permit selection of the amount of amplification desired, and dual or occasionally triple sensitivities are recorded to provide backup in case motion is not near the sensitivity level chosen. During FY78 a total of 483 surface measurements were made,

399 of which were recorded at a second sensitivity. There were 246 down-hole measurements, of which 222 were recorded at a second sensitivity. In addition, a substantial number of the over 230 measurements made for other programs have provided usable data to the data bank at no cost to the waste program. A listing of measurements by nuclear event or by stations is classified and is not included in this report. Some of the measurements made on smaller events were made to evaluate the limits of the amplified data and have provided data with a sufficiently small signal-to-noise ratio so as to be of questionable utility.

On the Purse event (U-20v) a seismic anomaly was observed in the vicinity of Engine Test Stand 2 in Jackass Flats; peak accelerations were five or more times greater than they were about 15,000 ft to the east, south, and west. The existence of an unexplained seismic "hot-spot" is of concern in the event the Jackass Flats area is used for a terminal waste storage facility. With an unexplained hot-spot there is a potential problem in satisfactorily answering an intervenor who asks, "How do you know there is not a similar hot-spot at another site under consideration?" One postulated mechanism for the hot-spot is that it results from a focusing, with the presumed granitic intrusion of Calico Hills serving as the focusing lens. U-20v is located N18.90 W of ETS-2. On that bearing ETS-2 is 11,973 ft from the axis of the Calico Hills aeromagnetic anomaly. (The peak of the anomaly is about 5990 ft to the east.) The bearing crosses the aeromagnetic anomaly axis at about N769,400; E600,586, which is taken as the focal point. It is the intent of the measurements described below to determine if the epicenter of the anomaly rotates about Calico Hills as the shot point is rotated. Measurements were made during FY78 on the Panir and Rummy events.

The assumed focal point is on an azimuth of 175.97° from the Panir event (Figure 2). At 11,973 feet from the focal point along that azimuth, the coordinates of the seismic anomaly center are N757,457; E601,428. Four stations were located along a tangent perpendicular to the azimuth to the ground zero. The coordinates of the stations are as follows:

Station A	N756,613	E589,458
Station B	N757,035	E595,443
Station C	N757,457	E601,428
Station D	N758,301	E613,398

There is 6000 feet between Stations A, B, and C, and 12,000 feet between C and D. Canisters were oriented toward ground zero (GZ).

The assumed focal point is on an azimuth of 224.90° from the Rummy event (Figure 1). At 11,973 feet from the focal point along that azimuth, the coordinates of the seismic anomaly center are N760,919; E592,135. Again, four stations were located along a tangent perpendicular to the azimuth to the ground zero. The coordinates of the stations are as follows:

Station A	N769,389	E583,635
Station B	N765,154	E587,885
Station C	N760,919	E592,135
Station D	N756,684	E596,385

There is 6000 ft between Stations. Canisters were oriented toward GZ.

Data Processing

After data have been digitized they are subjected to further processing. Figure 4 is a block diagram of the processing sequence. The following text describes the sequence using a letter keyed to the letter in the block diagram. Examples are shown in figures.

a. An auto-adjust plot is the first visual presentation of the data. The automatic adjustment causes the first and last points of the first integral of an acceleration record to be set to zero. Figure 5a is an acceleration

record; its auto-adjusted integral is shown in Figure 5b. Without the auto-adjustment, the departure of the acceleration base line from zero could cause the integral to be so large as to obscure the signal in the integral. This is shown in Figure 6.

b. Record repair is ordinarily performed on the record of the measurement rather than on the integral. For most repairs it is necessary to expand the time in the vicinity of the repair to be able to achieve the desired precision. The purpose is to salvage data which otherwise could not be put through the subsequent processing steps. Figure 7 shows the records in Figure 5 with the noise spikes removed. To see why the noise spike must be removed one may compare the integrals in Figures 5b and 7b at minus 5 s.

c. Arrival times represent the onset of the first signal and are determined from plots of acceleration with the time scale greatly expanded. Listings of acceleration-time aid in picking the arrival time more precisely.

d. Arrival time plotted against the slant range is useful when determining seismic velocity and determining whether arrivals are from direct or refraction paths.

e. Power spectra are plotted for the noise (o symbols in Figure 8) and for the signal plus noise (x symbols). The data are digitized from minus 1 min to provide resolution of noise frequencies as low as 0.1 Hz.

f. Where the two curves in Figure 8 separate defines where the signal emerges from the noise and is used to set the high-pass and low-pass frequency cut-offs required for the next step.

g. The Stearns Automated Method (SAM) is described in Figure 9. Ordinarily, digitized acceleration data are the input. Where velocity data are processed they are first differentiated and then treated as an acceleration record. This provides acceleration-time histories where acceleration was not measured directly. After sample decimation and high-pass filtering, the acceleration-time data are put on tape for later plotting. They are then put through a frequency domain integration and trend removal. After taking out any residual baseline shift, that output is put on tape for later plotting of velocity-time histories and is followed by another frequency domain integration. Removal of a parabola and baseline shift provides the displacement-time data, which also are put on tape for later plotting.

h. The output of the SAM procedure is used to plot acceleration, velocity, and displacement, each as a function of time (Figures 10, 11, and 12). If the plots appear satisfactory, processing moves to the next step. If not, it is usually because the frequency cut-offs chosen in Step f were not suitable. In order to achieve batch processing in Step g, a single value is chosen for high-pass frequency cut-off, a single value for low-pass cut-off, and a single value for the cut-off bandwidth (Δf) after examining spectra from all gages on a single nuclear event. These values are then used for all gages. This results in a compromise in some cases, and occasionally it later proves necessary to choose a different set to process a channel of data for which the general choice was not suitable.

i. Plots of 2- and/or 3-component vector-sums are made for acceleration, velocity, and displacement as functions of time. Peak 3-component vector-sum values were used for the Environmental Research Corporation (ERC) prediction

equations and for those developed herein, and it is this motion which is most appropriately applied in the response of underground structures. For surface structures, which are designed to be strong with respect to vertical forces, the 2-component vector-sums for the horizontal motion are often preferred. Either or both can be provided; Figures 13 and 14 illustrate acceleration. Similar plots are made for velocity and displacement; Figures 15 and 16 are for 3-component vectors.

j. Plots of Pseudo Relative Response Velocity (PSRV) can also be made (Figure 17). These are useful in that this is the form in which NRC usually specifies the structural response criteria which designs are required to meet.

k. For the analysis described later and the development of prediction equations, peak values from the 3-component vector-sum plots are tabulated together with the slant distance from the burst point to the sensor. The yield of the event is used for the multiple regression described later.

l. These peak values and distances then become part of a data set or subset used in prediction equations based on data from a number of events. Separate equations for single events are also examined to check on the internal consistency of the data from that event.

Past Prediction Methods

Prediction of ground motion prior to the current effort was based on equations developed by ERC from analysis of measurements made by the U.S. Geological Survey (USGS). The principal purpose of the equations was for

predicting off-site damage, and the locations of the measurements ranged from on-site to Las Vegas and beyond. The preponderance of the data was from the greater distances. Relatively close-in measurements were seldom made and were limited by the high frequency cut-off of the instruments being used. The equations had the form

$$A(W,R) = K\, W^{n} R^{-m}$$

where W is yield in kilotons, R is distance in kilometers, A is acceleration, and K, m, and n are constants determined from the data by regression analysis. The same form was used for acceleration, velocity, and displacement. The input of the ground motion parameters was the peak vector sum of the parameter. The ERC analysis divided the data into subsets according to whether the station was located on alluvium or rock and according to whether Yucca Flat shots were in alluvium or tuff and whether Pahute Mesa shots were in tuff or rhyolite. Their analysis does not include events after May 7, 1969; hence, data from the larger events of the accelerated test program of July 1974 to March 1976 were excluded.

It appeared that the prediction capability for the waste program could be improved over the ERC equations by using only data from on-site and near off-site locations, and by using measurements from yields closer to the maximum potential yields of the various test areas. When development of relationships with those restrictions is described below, the values from the earlier ERC equations will be included for comparison.

Current Development of Prediction Capability

Data Sets

There are three data sets corresponding to three testing areas. There is a high-yield data set for developing predictions for shots on Pahute Mesa where the potential maximum yield is considered to be about 1 Mt, an

intermediate-yield data set for Buckboard Mesa where the yield limit is about 700 kt, and a Yucca Flat data set where the upper limit would be about 250 kt. The latter limit would also apply to events in the Frenchman Flat region. For security reasons, the data have been scaled to the one of the above three yields associated with the data set.

When the work has been completed there will be prediction equations for acceleration, velocity, and displacement. Because acceleration is the primary parameter, we have chosen to prepare equations for it first. Only work done on acceleration is reported herein, although for many of the events the 3-component vector sums for velocity and displacement are completed also. When the decision was reached to discontinue work at the Eleana site, it was decided to concentrate first on the Pahute Mesa and Buckboard Mesa data sets and to work on the Yucca Flat data set at a lower priority.

Tables 2 and 3 list the events in each of the three data sets. It should be noted that the Buckboard Mesa data set is not made up of events fired in the Buckboard Mesa area, but rather of those fired on Pahute Mesa judged to be most appropriate for estimating ground motion in the event future shots are to be detonated in the Buckboard Mesa area.

The tables show also the source of the data, the number of stations for which three components of motion are available from each source, and the number of stations for which processing of acceleration data is complete. The last two columns summarize the number of stations for which acceleration processing has been completed and the number remaining to be done.

The question marks in the LASL data column of Table III merely indicate that the number of stations providing usable data has not been determined. The uncompleted Sandia data are from relatively recent events or from earlier events where the data require special treatment which takes additional time. There is a backlog of USGS data from their analog tapes for which digitizing was not completed during the fiscal year.

Analysis

For each of the data sets, the analysis has taken two forms. The first is a multiple regression analysis which provides a prediction equation in the same form as that used earlier by ERC. The second is to scale the data for each event to the maximum yield for the area of concern and to look for the event showing the greatest coupling and transmission and hence the strongest ground motion. In both cases a standard error of estimate was determined, which here will be referred to as sigma although that term is ordinarily used to denote standard deviation.

The Pahute Mesa data set alone is insufficient to yield a suitable prediction equation until more data are processed. The Buckboard Area data set yields the following:

$$a = 0.137\ W^{0.704}\ R^{-1.75};\ \sigma_a = 1.81,\ \sigma_R = 1.40; \qquad (1)$$

where

a = peak acceleration in g
W = yield in kt
R = slant distance in km

If the Pahute Mesa and Buckboard Area data sets are combined, the following equation results:

$$a = 0.355\ W^{0.526}\ R^{-1.73};\ \sigma_a = 1.83,\ \sigma_R = 1.42. \qquad (2)$$

There is essentially no change except for the intercept and yield dependence, and those changes are small.

The corresponding ERC equation may be compared with the above.

$$a = 0.249\ W^{0.465}\ R^{-1.34};\ \sigma_a = 2.30,\ \sigma_R = 1.86. \qquad (3)$$

The smaller exponent on radial distance results from the inclusion of data from the distant off-site stations where motion amplitudes are relatively large. The larger sigma values are in part a result of having included data from events covering a wider range of yields and geological settings.

Table 4 lists the distances in kilometers to 0.7, and to 0.5 g, and shows the mean and sigma 1, 2, 3, and 4 values. Thus, it can be seen that distances are significantly reduced, especially for the higher sigma levels.

The Yucca Flat data set provides the following equation:

$$a = 0.265\ W^{0.465}\ R^{-1.53};\ \sigma_a = 2.16,\ \sigma_R = 1.65. \qquad (4)$$

The comparable ERC equation is:

$$a = 0.0903\ W^{0.588}\ R^{-1.37};\ \sigma_a = 2.26,\ \sigma_R = 1.81. \qquad (5)$$

Differences between the predictions using the two equations are quite small. It is expected that the results may change for Eq. (4) as additional data in the set are processed and added. Whether or not this changes the predictions significantly remains to be seen.

The value of sigma derived from the equations results from the scatter in the data from which they were derived. The scatter results from a number of factors, and it is necessary that the reader understand what

each factor is, how much it contributes to the scatter, and what (if anything) can be done to reduce the scatter.

Distance -- Locations of close-in stations and surface ground zeros are surveyed to fractions of a foot. Locations of some of the more distant stations are given to the nearest second or 1/100 minute. Slant distances between explosion source are calculated taking into account the elevation of surface GZ, the depth of the working point, and the elevation of the station. The contribution of distance to the scatter is insignificant as long as the data have been recorded correctly.

Yield -- Yields are most often quoted as ±10%. This has no rigorous statistical meaning. Confidence in yield determination is a function of the device design and the diagnostic measurements made. For some events there is accuracy greater than 10% and for some, less. It was a subjective judgment of those responsible for yield determination at LASL and LLL that the ±10% represents roughly a 1 sigma value.

Coupling -- The effectiveness with which the explosion energy is coupled to the earth is a function of medium properties in the immediate vicinity of the explosion. Events detonated in granite couple energy very well while those in dry porous media show considerable decoupling. Those detonated in dry alluvium are not well coupled. Coupling is increased when the shot point is below the water table. There is no quantitative evaluation of the variation in coupling, but some further attention is given to it below. An effort has been made to reduce the variation for shots fired in Yucca Flat by restricting the data set to shots fired in tuff below the water table.

Transmission -- Motion close to the shot is essentially in the form of a compression wave. At around two shot depths from surface zero, refracted waves begin to appear. At larger distances the wave train at the surface is made up of refracted signals arriving from many different paths; usually those refracted waves traveling through a high velocity, deeper structure arrive first, followed by surface waves. As might be expected, there is considerable azimuthal variation. For example, Boxcar,

which had stations at a number of azimuths, shows σ_a = 1.49, while Muenster, with all measurements in a single direction, had σ_a = 1.16.

Station Site Medium -- Peak ground motion amplitude also depends on the medium at the point of measurement. Typically, a station located on alluvium records greater amplitudes than one located at a comparable distance on hard rock. Two pairs of stations examined show that peak accelerations at an alluvium site are up to three times those at a hard rock site. For the close stations where the motion is strong, this difference is not significant, but it increases in importance with increasing distance. Here is a clear opportunity to reduce sigma further by using only data from stations on alluvium or hard rock according to whether a storage site in alluvium or hard rock is being considered.

Number of Stations -- When data for separate shots are considered individually there appears to be an increase in sigma with an increase in the number of stations at which measurements were made. It is not possible to separate this as an independent variable because an increase in the number of stations usually means an increase in the number of azimuths on which measurements are made, an increase in the number of transmission paths involved, and an increasing probability that some stations are located on both alluvium and hard rock.

Instrumentation -- Some of the scatter in data can be caused by instrumentation variations. The largest factor in instrument variation has to do with the accuracy of gage calibration and the stability of the calibration with time subsequent to the laboratory calibration. Accelerometers are given a ± 1 g field check prior to every use, but small departures from 1 g can be detected only in a laboratory calibration. No analysis of calibration effects on accuracy has been made in connection with this program. An analysis made of accelerometers used for close-in measurements on a prior program showed that peak velocity from integration of acceleration records had 50% of the measurements fall with 4% of the peak velocity measured.

Conclusions

The significance of the work to date can be illustrated by plotting some of the results shown in Table 4 on an NTS map. Let us assume that Calico Hills is a potential candidate site for a repository. Figure 18 shows a portion of NTS with Calico Hills in the lower left corner. A short dashed line shows the southern portion of the Buckboard Area as defined by USGS, indicating the closest points to Calico Hills at which 700 kt could be detonated. For a facility at Calico Hills designed to withstand 0.7 g, circles have been drawn about that point using the results of Eqs. (1) and (3) from Table 4. The solid circles are for Eq. (1) and the dashed circles are for the old ERC criteria from Eq. (3). Circles are shown for mean, 1σ, 2σ, 3σ, and 4σ (Eq. (1) only). These correspond to probabilities of 50%, 31.7%, 4.6%, 0.3%, and 0.005% that the 0.7-g level will be exceeded. Thus, the probability of a 700-kt explosion at the southern edge of the Buckboard Mesa Area producing more than 0.7 g at Calico Hills is considerably less than 0.3% based on the more recent analysis. This indicates that Calico Hills is a suitable site for a waste facility from the standpoint of compatibility with nuclear weapons testing if the facility is designed to withstand 0.7 g and licensing does not require more than a 3σ probability of exceeding the design acceleration. The corresponding level for the older ERC equations would be slightly above the 2σ probability. Clearly, the newer analysis presents a more optimistic estimate of the compatibility of a waste facility at the NTS with the nuclear weapons testing program.

TABLE 1

Seismic Measurements for a Terminal Waste Storage Program

Station	Location	Hole No.	Coordinates		Elevation (ft)	Medium	Date Installed
			North	East			
1	Area 16	None	840,515	634,760	Surf. ~5325	Eleana	8/77 (Removed 11/77)
2	Syncline Ridge	None	~843,250	~646,250	Surf. ~4785	Limestone over Eleana	8/77 (Removed 6/78)
3	Piledriver	Ue-15.01	901,147	677,016	Surf. 5036	Alluvium over Granite	9/77
					Tun. 3669 (1367)	Granite	9/77
4	Area 6	Ue-6b	810,000	678,450	Surf. 3933	Alluvium	4/77
					Hole 3505 (428)	Alluvium	4/77 (Removed 5/78)
5	Skull Mtn	None	~743,950	~633,150	Surf. ~4563	Tuff	10/77
6	ETS-2	None	758,073	604,467	Surf. ~3810	Alluvium	10/77
7	Calico Hills	None	~770,300	~607,100	Surf. ~4390	Eleana	10/77
8	Yacht Hole	Ue-1L	837,000	654,001	Surf. ~4465	Alluvium over Eleana	11/77 (Removed 8/78)
					Hole ~2265 (2228)	Eleana	3/78
9	Rainier Mesa	U-12g.08 CH No. 1	882,173	633,268	Surf. 7602.2	Tuff	12/77
					Tun. 6186.15 (1416)	Tuff	12/77
10	Well J-11	J-11	740,968	611,764	Surf. 3442	Alluvium	3/78
					Hole ~2116 (1329)	Tuff	3/78
10'	200	J-11'	~740,990	~611,764	Hole 3245 (200)	Alluvium	3/78
11	Area 4	Ue-4aa	854,145	666,794	Surf. 4210	Alluvium	3/78
					Hole 3076 (1134)	Limestone	3/78

TABLE 1 (cont)

Station	Location	Hole No.	Coordinates North	Coordinates East	Elevation (ft)	Medium	Date Installed
12*							
13	Area 18	Ue-18r	868,100	564,707	Surf. 5538 Hole 3038 (2500)	Tuff Welded Tuff	6/78 8/78
14	Yucca Mtn	None	~764,900	~568,400	Surf. 4070	Tuff	10/78
15	Dome Mtn	None	~813,804.34	~579,415.83	Surf. 6193	Lava	10/78
16	Forty-mile Canyon	None	~810,000	~585,600	Surf. 4200	Rhyolite	10/78
17	N. Timber Mtn	None	~850,800	~560,200	Surf. 7422	Tuff	7/78
18	S. Timber Mtn	None	~833,950	~557,896	Surf. 7239	Tuff	7/78
19*							

*Reserved for an unspecified future installation.

TABLE 2

Status of Data Processing and Analysis --
Pahute Mesa and Buckboard Mesa Area

	Sandia Data	USGS Digital	USGS Analog	LASL Data	Summary Finished	Summary Unfinished
			Pahute Mesa Data Set			
Boxcar	Complete 10	Complete 4	--	--	14	0
Camembert	Complete 6	--	1	--	6	1
Colby	9	--	--	--	0	9
Fontina	7	--	1	--	6	8
Hardley	Complete 6	--	3	--	6	3
Jorum	Complete 6	--	7	--	6	7
Kasseri	Complete 7	--	1	--	7	1
Muenster	Complete 6	--	1	--	6	1
					45	30
			Buckboard Mesa Area Data Set			
Almendre	Complete 6	Complete 16	5	--	22	5
Backbeach	10	--	--	3	7	6
Camenbert	Complete 6	--	1	--	6	1
Cheshire	Complete 6	--	1	--	6	1
Estuary	Complete 5	--	2	--	5	2
Fondutta	18	--	--	--	9	9
Halfbeak	Complete 6	Complete 4	--	--	10	0
Inlet	Complete 7	--	1	--	7	1
Kasseri	Complete 7	--	1	--	7	1
Mast	Complete 7	--	1	--	7	1
Muenster	Complete 6	--	1	--	6	1
Parir	23	--	--	--	0	23
Pool	11	--	Complete 4	--	4	11
Scotch	Complete 5	Complete 1	--	--	6	0
Tybo	Complete 10	--	--	--	10	0
					112	62

TABLE 3

Status of Data Processing and Analysis -- Yucca Flat

	Sandia Data	USGS Digital	USGS Analog	LASL Data	Summary Finished	Summary Unfinished
			Yucca Data Set			
Agile	10	--	--	--	0	10
Bulkhead	Complete 19	--	--	--	19	0
Chiberta	6	--	--	--	0	6
Commodore	10	--	Complete 1	--	1	10
Coulommiers	Complete 12	--	--	--	12	0
Escabosc	Complete 9	--	Complete 1	--	10	0
Esrom	2	--	--	--	0	2
Fardallones	16	--	--	--	4	12
Iceberg	25	--	--	?	0	25
Keelson	Complete 6	--	--	--	6	0
Latir	Complete 7	--	Complete 3	--	10	0
Marsilly	19	--	--	--	2	17
Miera	Complete 4	1	Complete 5	--	9	1
Mizzen	9	--	--	--	0	9
Oscuro	Complete 4	Complete 1	--	--	5	0
Portmanteau	Complete 6	--	--	--	6	0
Reblochon	Complete 8	--	--	--	8	0
Rudder	Complete 14	--	--	Complete 4	18	0
Rummy	21	--	--	?	0	21
Sandreef	Complete 4	--	--	?	4	0
Scantling	Complete 4	--	--	Complete 3	7	0
Starwort	Complete 3	Complete 5	--	--	8	0
Strait	Complete 4	--	7	--	4	7
					133	120

TABLE 4

Distances (km) to Given Ground Motion Levels

Peak Acceleration	Sigma	Equation 1	Equation 2	Equation 3
0.7 g	Mean	5.39	4.98	4.49
	1	7.70	7.17	8.85
	2	11.01	10.32	15.54
	3	15.75	14.87	28.90
	4	22.52	21.41	53.75
0.5 g	Mean	6.54	6.05	5.77
	1	9.35	8.72	10.74
	2	13.36	12.55	19.97
	3	19.11	18.09	37.14
	4	27.33	26.03	69.09

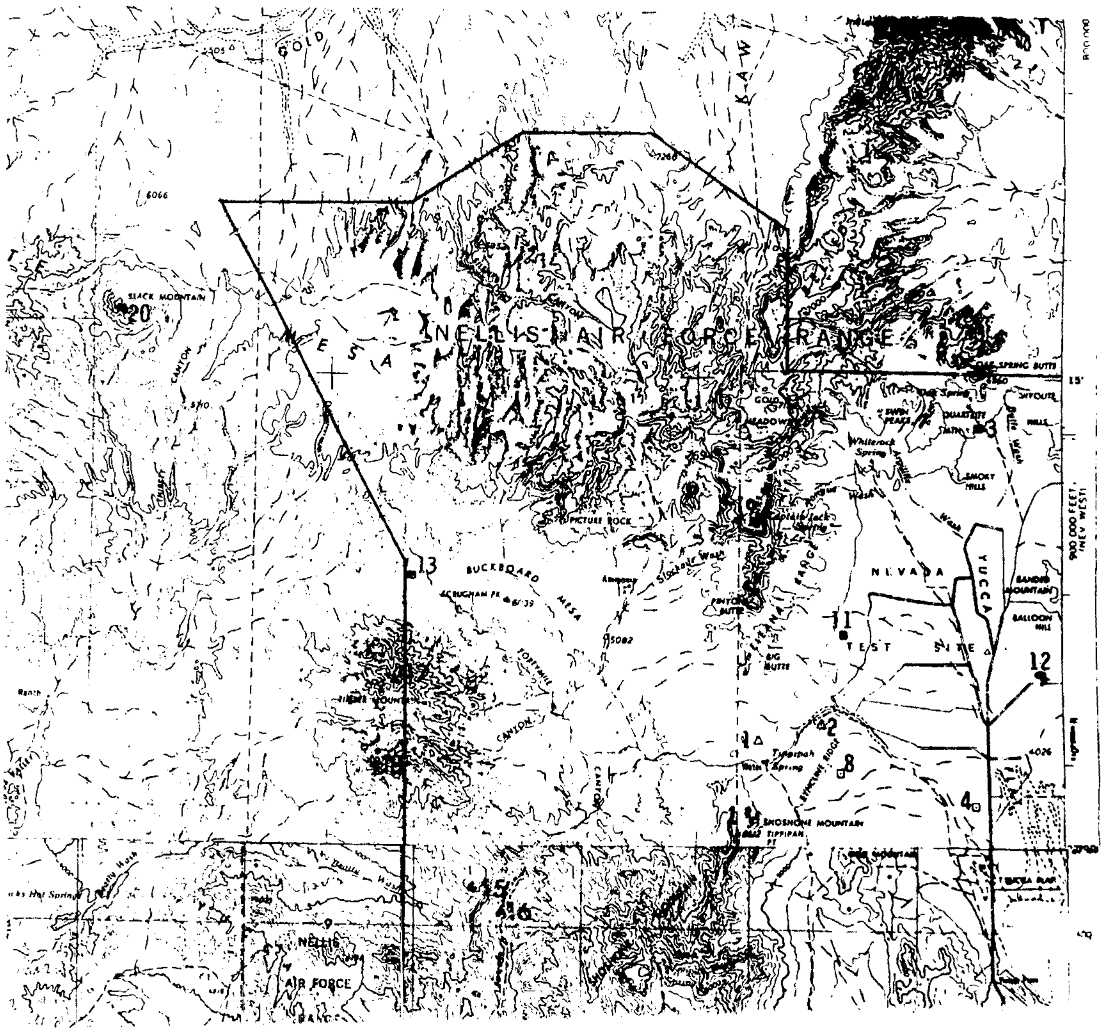

GOLD
NELLIS AIR FORCE RANGE
MESA
20
13
BUCKBOARD MESA
PICTURE ROCK
CANYON
FORTYMILE
Slockade Wash
NEVADA TEST SITE
YUCCA
11
12
2
8
4
3
Tippipah Spring
SHOSHONE MOUNTAIN
15
16
NELLIS AIR FORCE
5082
6066
900 000 FEET (NEV WEST)

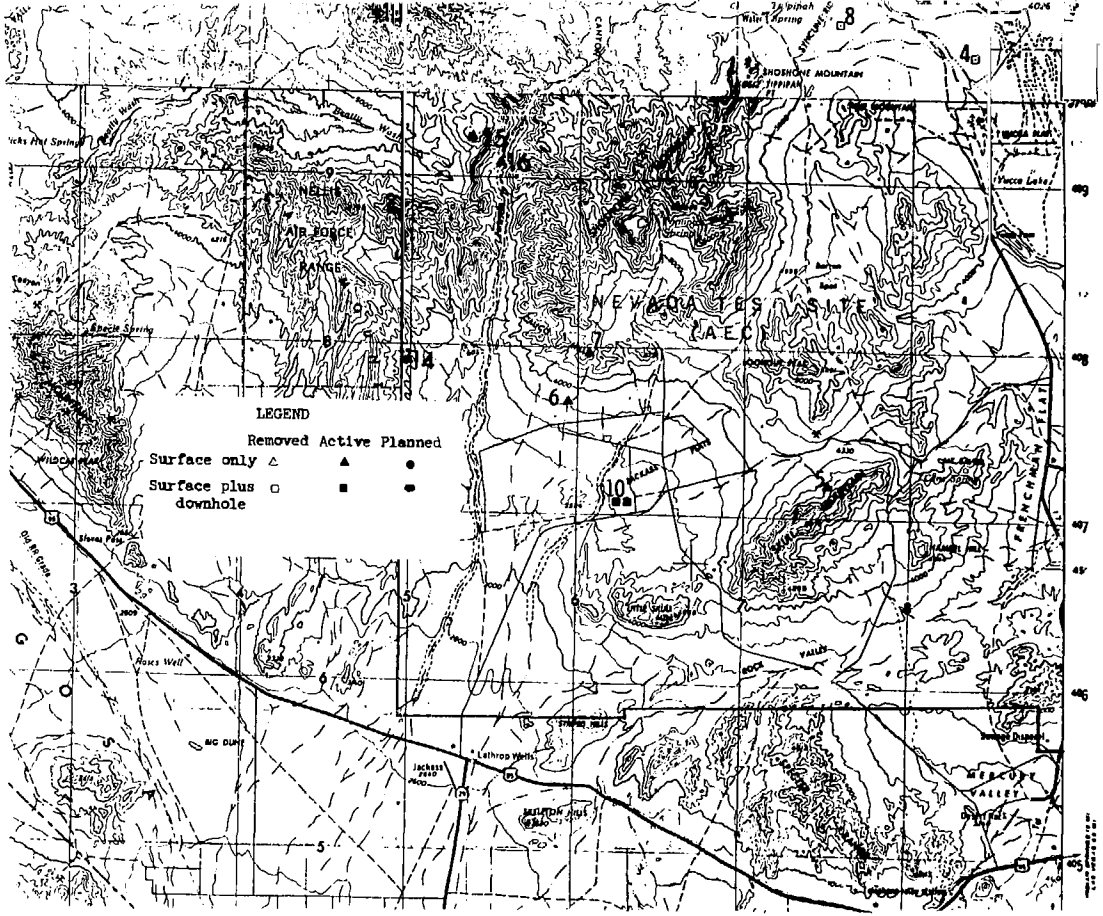

Figure 1. Location of Stations Where Ground Motion Measurements Are Being Made

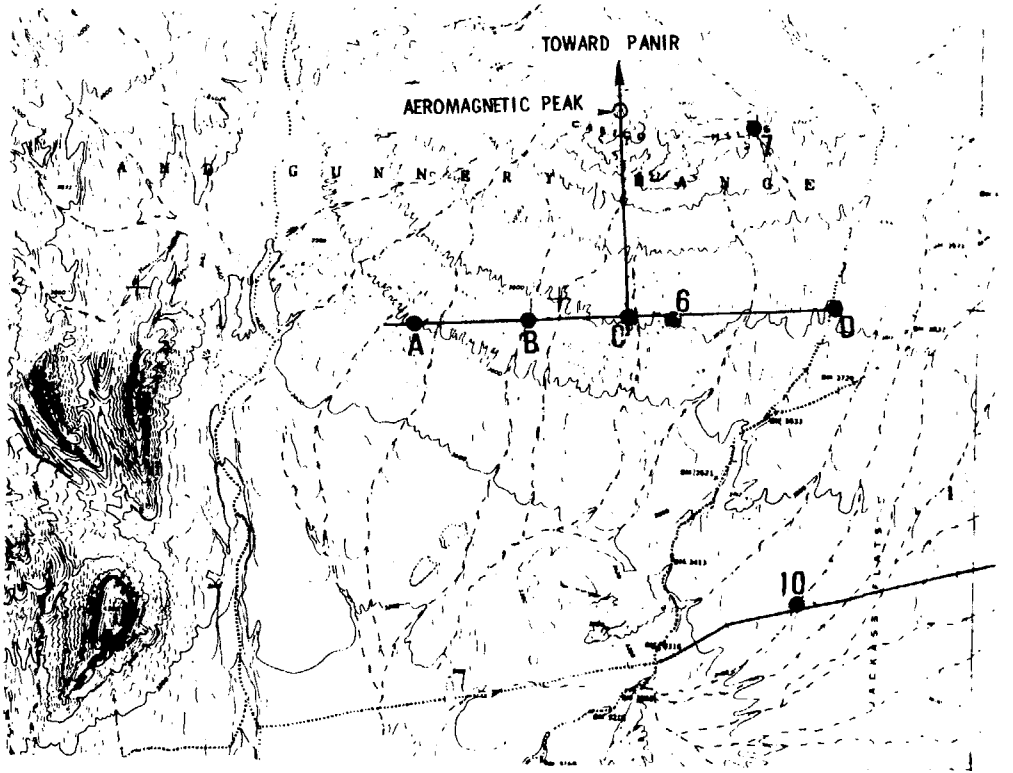

Figure 2. Station locations for Panir Event

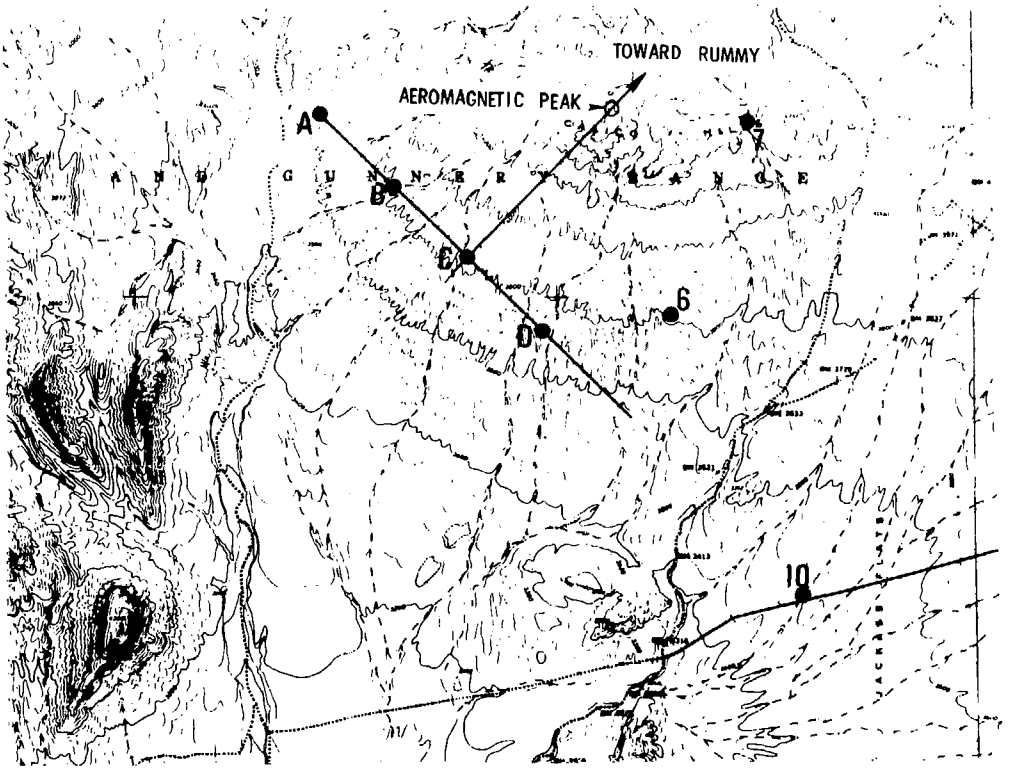

Figure 3. Station Locations for Rummy Event

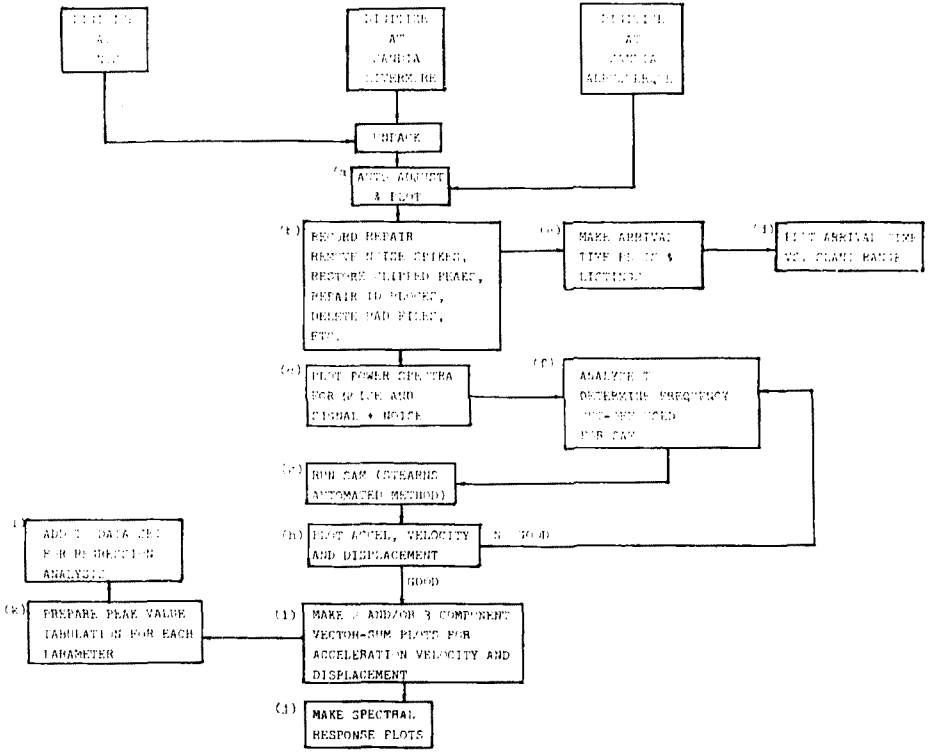

Figure 4. Block Diagram of Data Processing Sequence

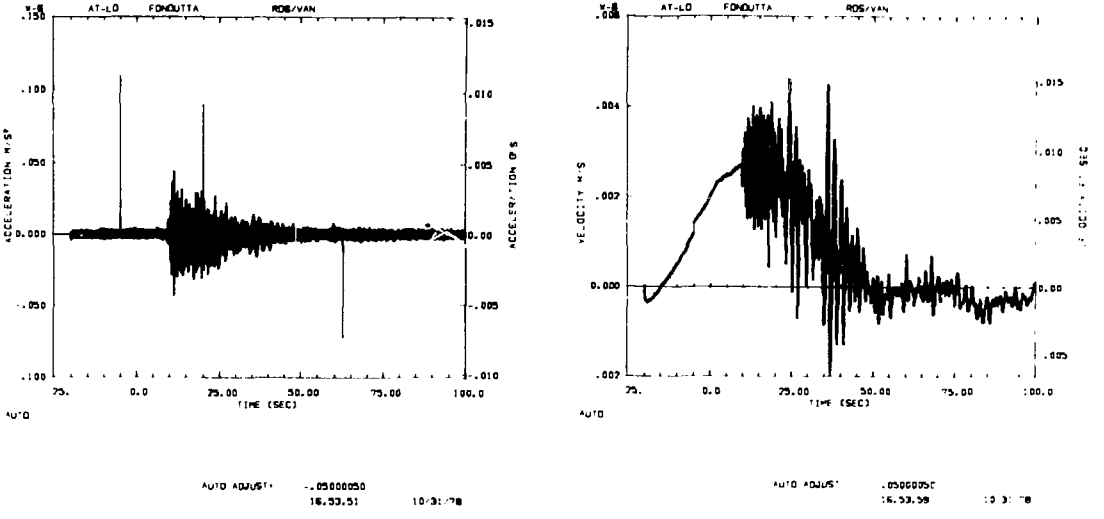

(a) (b)

Figure 5. Acceleration Record and Its Auto-Adjusted Integral from Fondutta Event

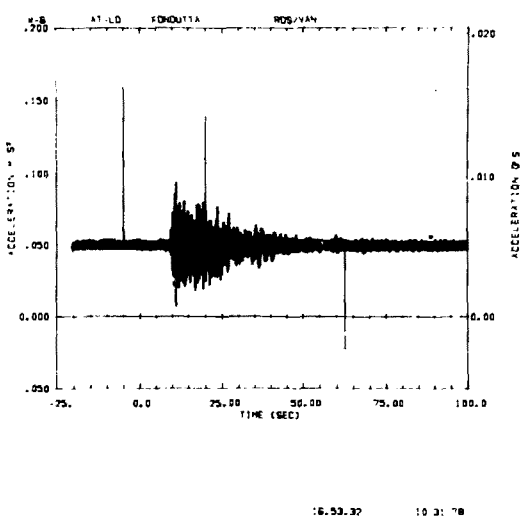

(a)

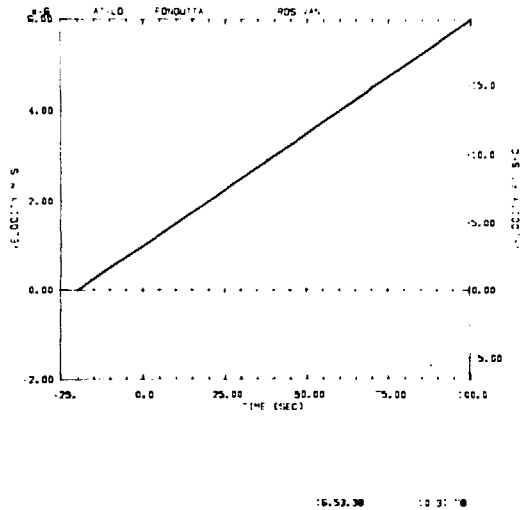

(b)

Figure 6. Acceleration and Velocity vs Time for Fondutta Event

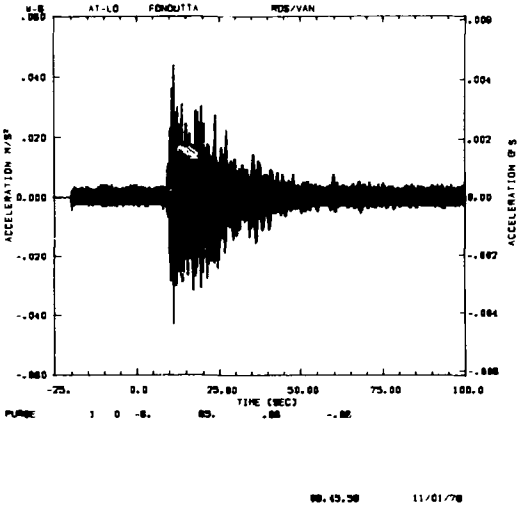

(a)

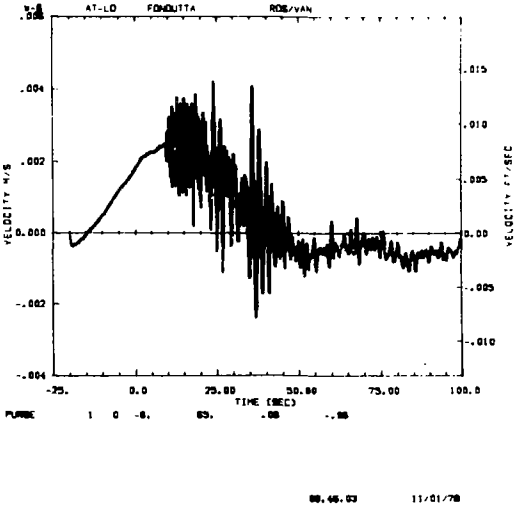

(b)

Figure 7. Acceleration Record and Its Auto-Adjusted Integral from Fondutta Event With Noise Spikes Removed

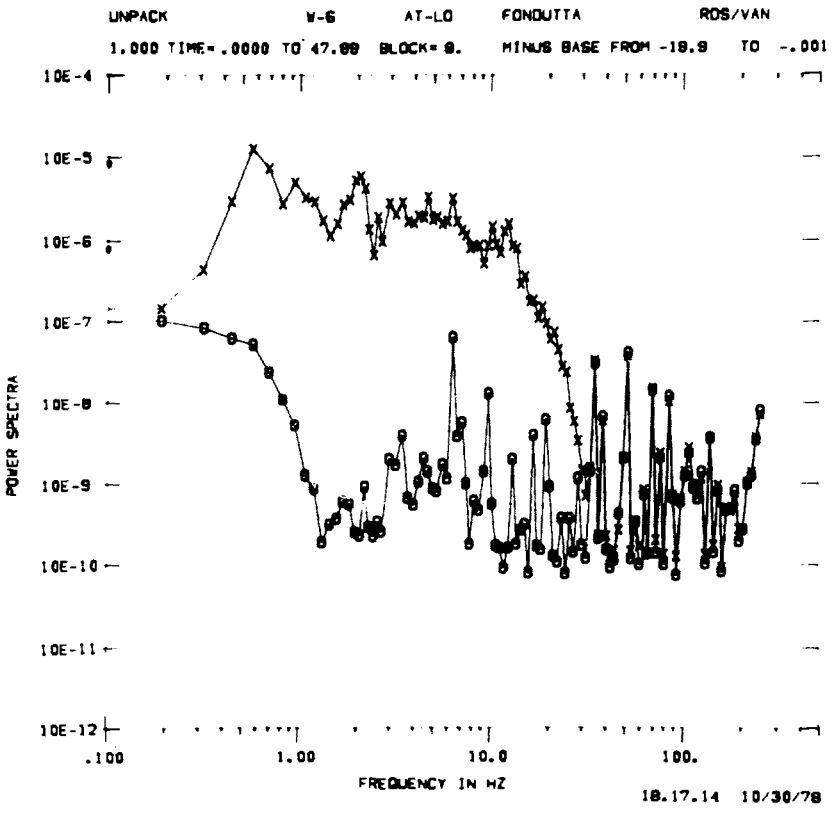

Figure 8. Power Spectra vs Frequency for Fondutta Event

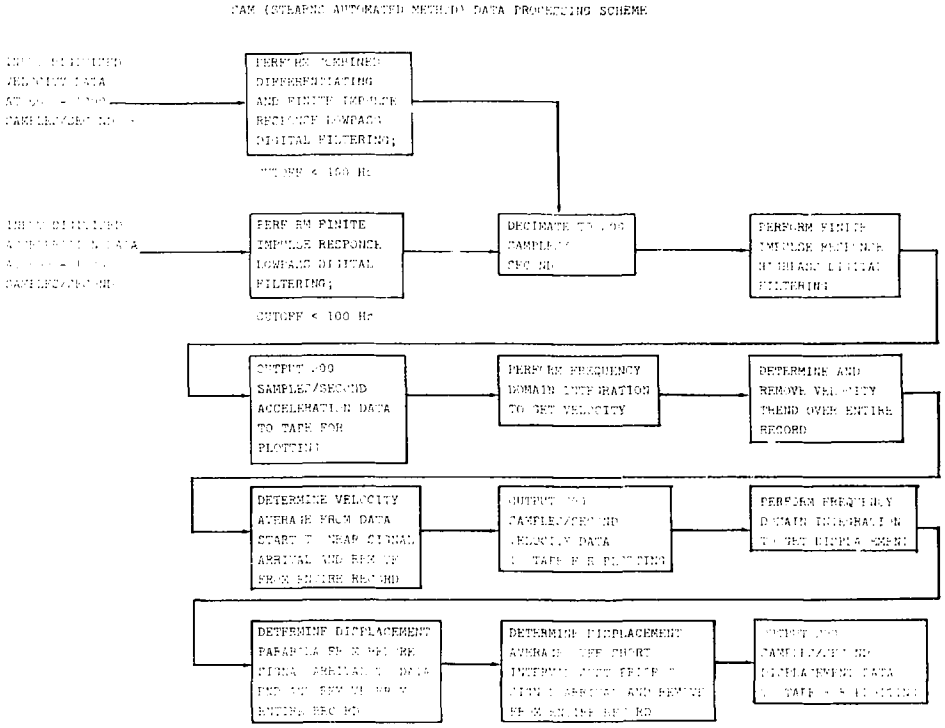

From SAND77-1643, Integration and Interpolation of Sampled Waveforms, S. D. Stearns, January 1978, Sandia Laboratories, Albuquerque NM

Figure 9. SAM Data Processing Scheme

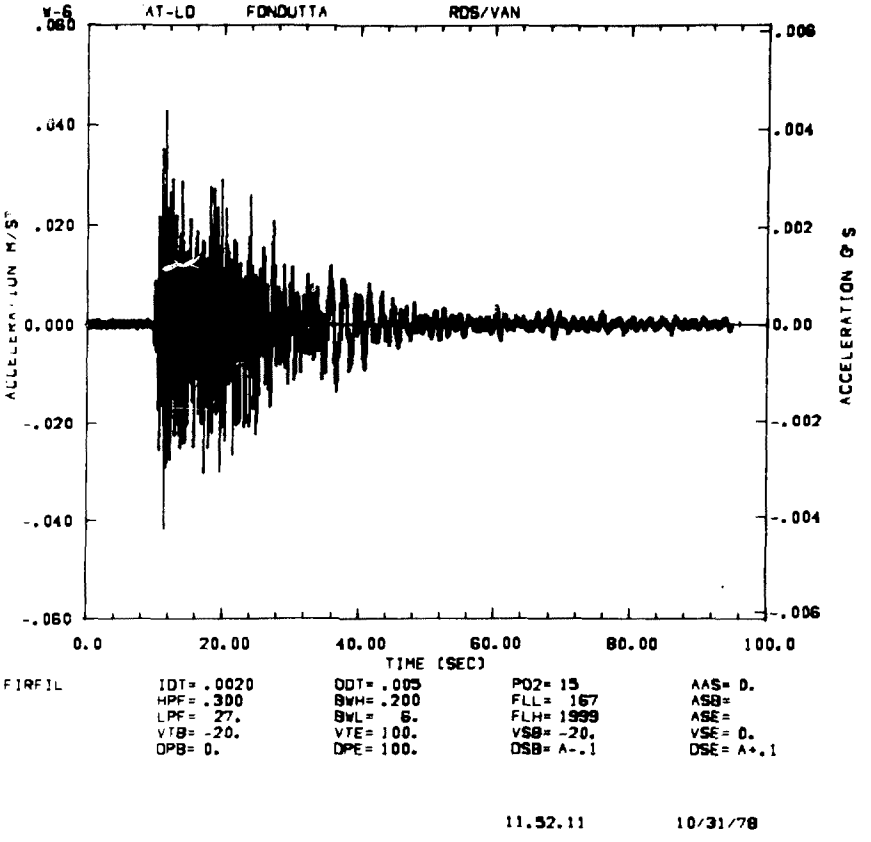

Figure 10. Acceleration vs Time for Fondutta Event

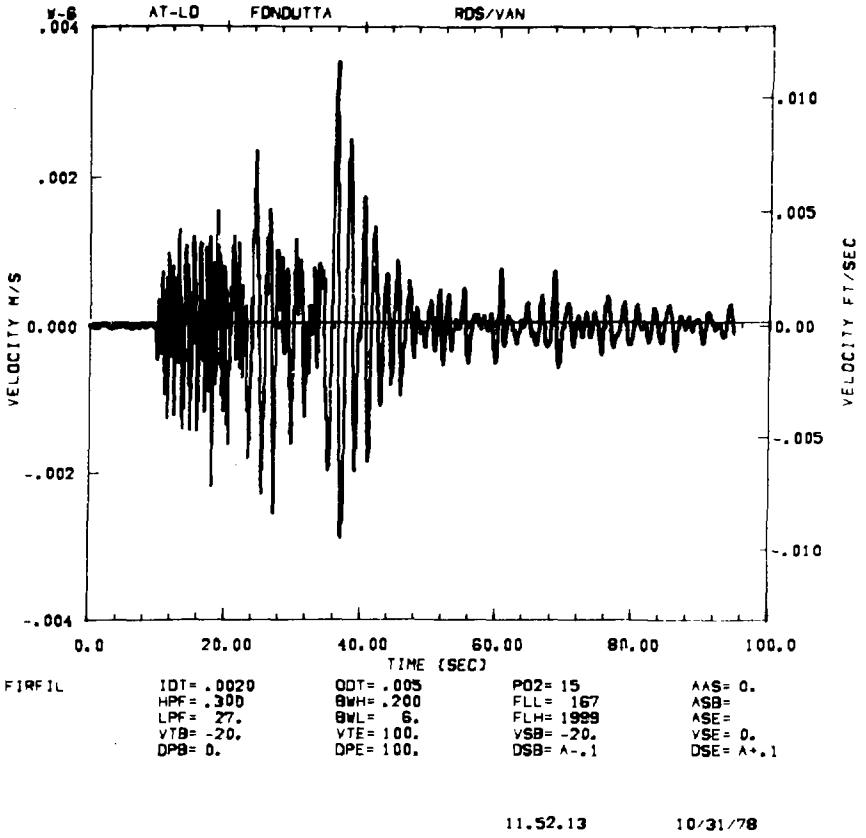

Figure 11. Velocity vs Time for Fondutta Event

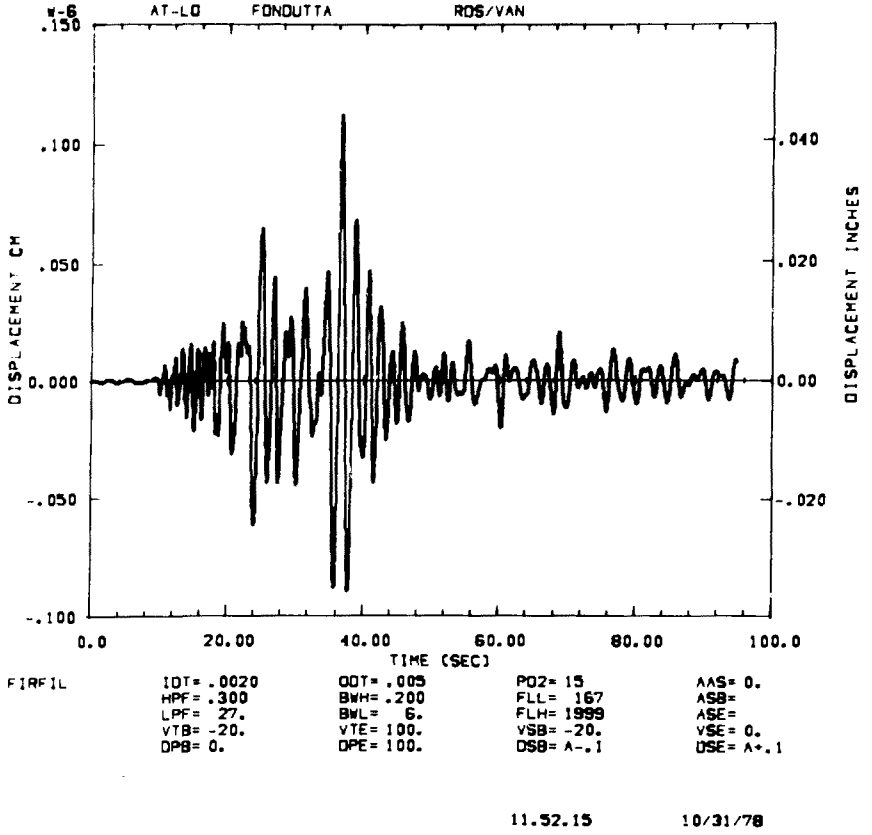

Figure 12. Displacement vs Time for Fondutta Event

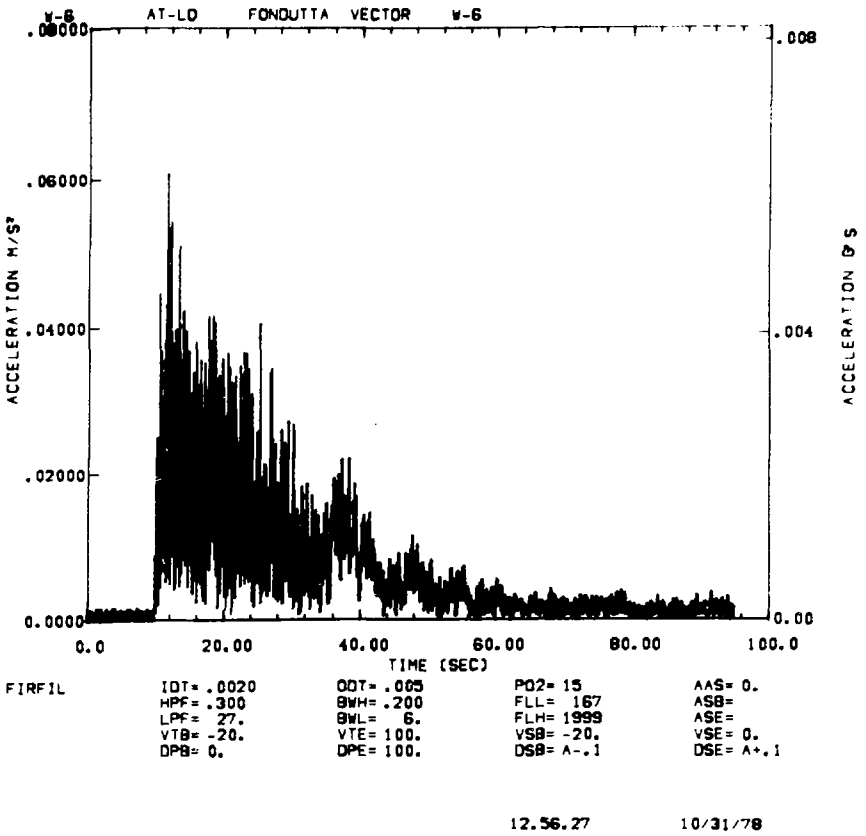

Figure 13. Three-Component Acceleration Vector-Sum for Fondutta Event

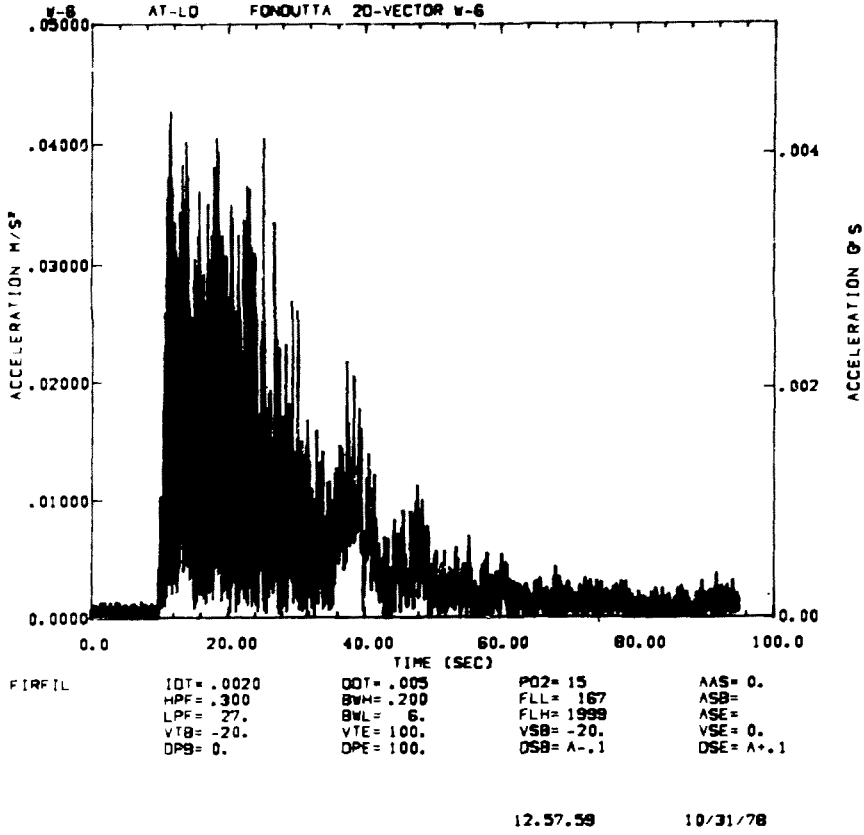

Figure 14. Two-Component Acceleration Vector-Sum for Fondutta Event

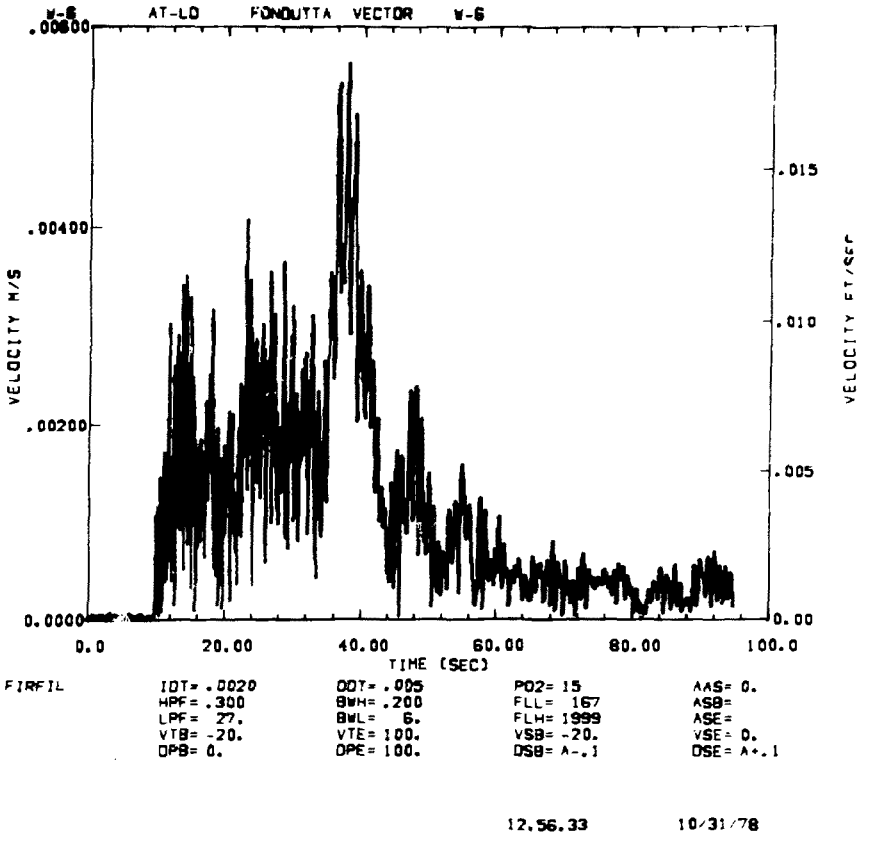

Figure 15. Three-Component Velocity Vector for Fondutta Event

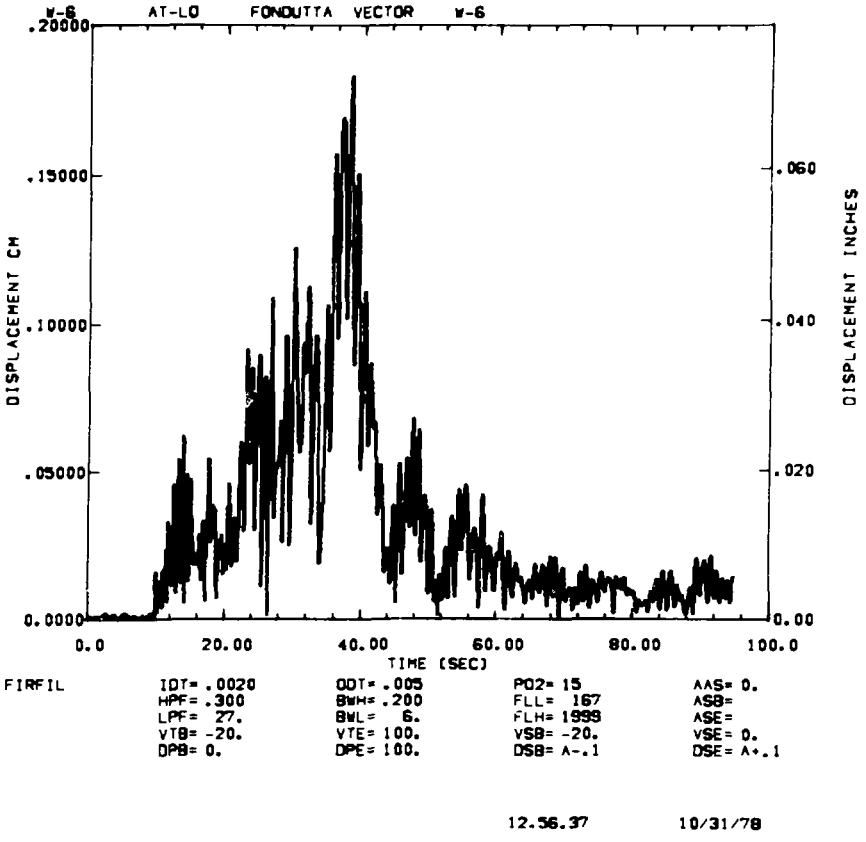

Figure 16. Three-Component Displacement Vector for Fondutta Event

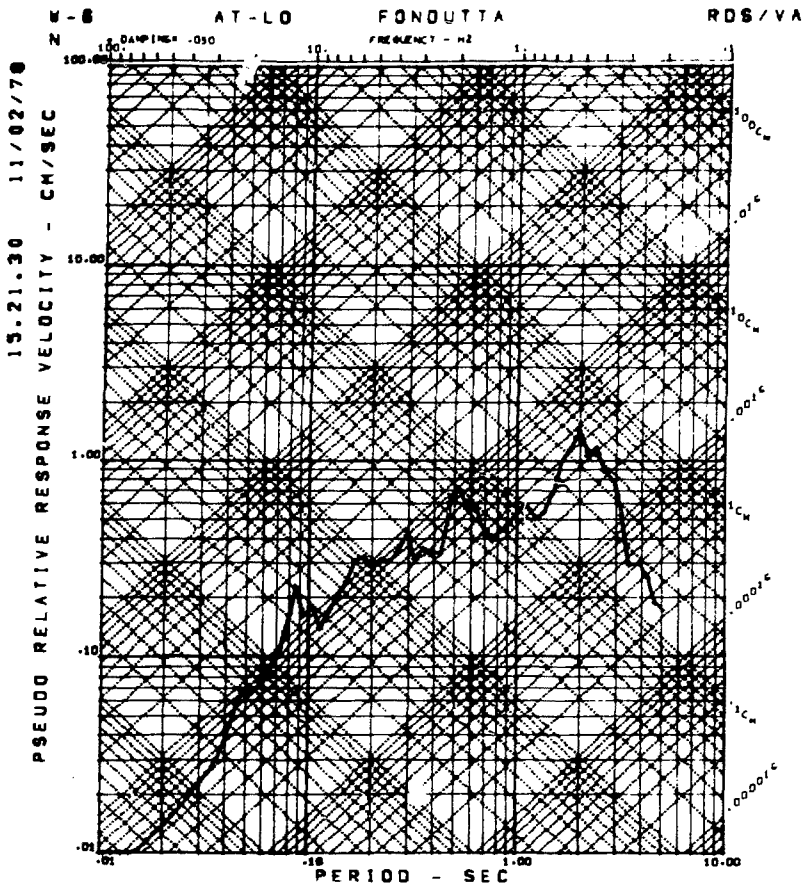

Figure 17. Pseudo Relative Response Velocity for Fondutta Event


Equation 1
Equation 3
3σ
4σ
3σ
2σ

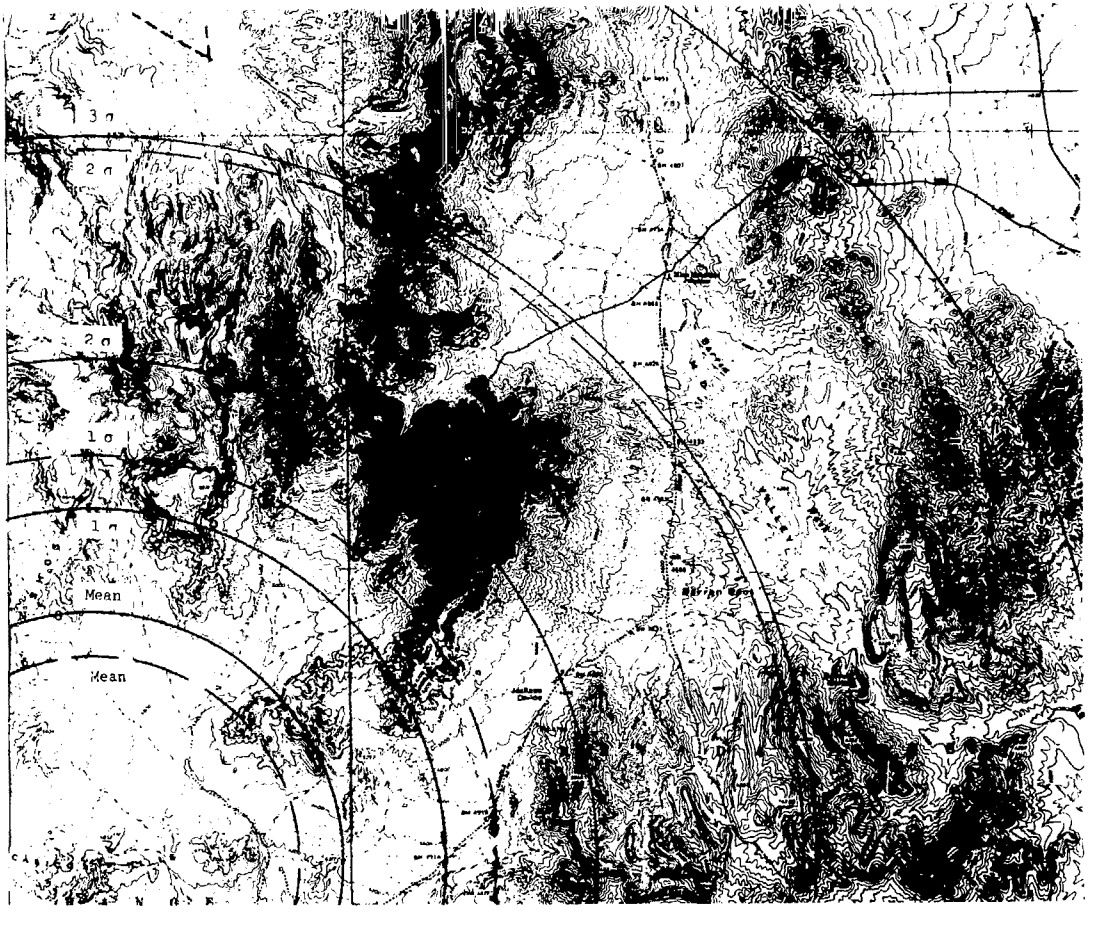

Figure 18. Mean and 1-, 2-, 3-, and 4-σ Levels for Storage Facility at Calico Hills, NTS